

# RSC Advances



This is an *Accepted Manuscript*, which has been through the Royal Society of Chemistry peer review process and has been accepted for publication.

*Accepted Manuscripts* are published online shortly after acceptance, before technical editing, formatting and proof reading. Using this free service, authors can make their results available to the community, in citable form, before we publish the edited article. This *Accepted Manuscript* will be replaced by the edited, formatted and paginated article as soon as this is available.

You can find more information about *Accepted Manuscripts* in the [Information for Authors](#).

Please note that technical editing may introduce minor changes to the text and/or graphics, which may alter content. The journal's standard [Terms & Conditions](#) and the [Ethical guidelines](#) still apply. In no event shall the Royal Society of Chemistry be held responsible for any errors or omissions in this *Accepted Manuscript* or any consequences arising from the use of any information it contains.

# Azopyridine-Functionalized Benzoxazine with $Zn(ClO_4)_2$ Form High-Performance Polybenzoxazine Stabilized Through Metal–Ligand Coordination

Mohamed Gamal Mohamed,<sup>a</sup> Wei-Chen Su,<sup>a</sup> Yung-Chih Lin,<sup>a</sup> Chih-Feng Wang,<sup>d</sup> Jem-Kun Chen,<sup>e</sup> Kwang-Un Jeong,<sup>f</sup> and Shiao-Wei Kuo<sup>a,b,c\*</sup>

Received (in XXX, XXX) Xth XXXXXXXXX 200X, Accepted Xth XXXXXXXXX 200X

DOI: 10.1039/b000000x

In this study we prepared a benzoxazine monomer (Azopy-BZ) featuring azobenzene and pyridine units through the reaction of paraformaldehyde, aniline, and 4-(4-hydroxyphenyleazo)pyridine (Azopy-OH), itself obtained through a diazonium reaction of 4-aminopyridine with phenol in the presence of sodium nitrite and NaOH. The azobenzene and pyridine groups in the benzoxazine monomer were played to roles: (i) allowing photoisomerization between the planar trans form and the nonplanar cis form of the azobenzene unit (characterized using UV–Vis spectroscopy and contact angle analyses) and (ii) serving as a catalyst that accelerated the ring opening polymerization of the benzoxazine units, where the exothermic peak shifted to lower temperature during differential scanning calorimetry (DSC) analyses. The curing temperature of the model benzoxazine 3-phenyl-3,4-dihydro-2*H*-benzoxazine (Pa-type) was 263 °C; it decreased to 208 °C for Azopy-BZ, presumably because of the basicity of the azobenzene and pyridine groups. Blending with zinc perchlorate [ $Zn(ClO_4)_2$ ] not only improved the thermal properties, as determined through dynamic mechanical analysis (DMA), due to physical crosslinking of the pyridine units through zinc cation coordination in a metal–ligand bonding mode, but also further facilitated the ring opening polymerization to occur at a temperature of only 130 °C (DSC). Thus, the presence of this  $Zn(ClO_4)_2$  overcame the problem of high temperature curing (ca. 180–210 °C) required of traditional polybenzoxazines. Introducing the azobenzene and pyridine units and the zinc salt into this polybenzoxazine system provided a multifunctional material that exhibited photoisomerization-based tuning of its surface properties, accelerated ring opening polymerization of its oxazine rings, and increasing physical crosslinking density, through metal–ligand interactions, to enhance its thermal properties.

## Introduction

1,3-Benzoxazines are receiving considerable attention because of their promising practical applications as monomers for high performance materials.<sup>1–6</sup> Their facile and versatile syntheses from relatively abundant materials (e.g., phenols, amines, formaldehyde) is also attractive from the viewpoint of developing novel benzoxazines bearing a variety of functional groups.<sup>7–17</sup> Some of these functional groups serve as reactive sites to increase the degree of crosslinking, thereby varying the thermal and mechanical properties of the obtained polybenzoxazines to fulfill specific requirements. Because the chemical structure of a polybenzoxazine is similar to that of a traditional phenolic resin, polybenzoxazines possess good heat resistance, flame retardance, good mechanical properties, low dielectric constant, dimensional stability, low water absorption, and low surface free energy.<sup>1,18–26</sup> As a result, polybenzoxazines have potential uses as matrix resins for carbon fiber-reinforced plastics, adhesives, and electronic materials (e.g., rigid printed circuit boards). Nevertheless,

polybenzoxazines do have some unattractive properties, including high curing temperatures for their ring opening polymerizations, brittleness, and moderate glass transition temperatures ( $T_g$ ) that are not sufficiently high for applications under harsh conditions.<sup>1,23,27</sup> Many approaches have been reported to overcome these shortcomings. For example, the mechanical and thermal properties of the benzoxazine can be improved significantly after blending with various polymers (e.g., epoxy,<sup>28,29</sup> polyurethane,<sup>30,31</sup> polyimide<sup>32</sup>) or through copolymerization. In addition, the preparation of specifically designed novel polybenzoxazines or high-molecular-weight benzoxazines featuring another polymerizable group (e.g., ethynyl,<sup>33</sup> phenylethynyl,<sup>34</sup> nitrile,<sup>35</sup> propargyl,<sup>36</sup> allyl<sup>37</sup>) or hydrogen bonding functional group<sup>38,39</sup> can be an effective means of enhancing the thermal properties.

Another application of functionalized benzoxazine monomers is their combination with inorganic materials (e.g., clay,<sup>40–42</sup> polyhedral oligomeric silsesquioxane (POSS),<sup>43–47</sup> carbon nanotubes,<sup>48,49</sup> graphene<sup>50</sup>) to fabricate nanocomposites, stabilized through attractive interactions between the polar functional groups of the monomer units and the inorganic surfaces. For example, Yagci et al. demonstrated the surface functionalization of magnetite nanoparticles with a benzoxazine bearing a carboxyl moiety; they also developed a polybenzoxazine/montmorillonite nanocomposite by using a benzoxazine bearing a 4-pyridyl moiety as a key material.<sup>40,41</sup>

Combining metal ions with benzoxazines is also an interesting means of preparing new high-performance polybenzoxazines. Endo et al. reported a novel 1,3-benzoxazine bearing a 4-aminopyridyl moiety, synthesized from 4-aminopyridine, *p*-cresol, and paraformaldehyde, with acetic acid added to neutralize the basicity of the system. The introduction of the 4-aminopyridyl moiety resulted in a polymer exhibiting high affinity toward metal ions [e.g., copper(II), cobalt(II)], leading to

<sup>a</sup>Department of Materials and Optoelectronic Science, National Sun Yat-Sen University, Kaohsiung, Taiwan.

<sup>b</sup>Department of Medicinal and Applied Chemistry, Kaohsiung Medical University, Kaohsiung, Taiwan.

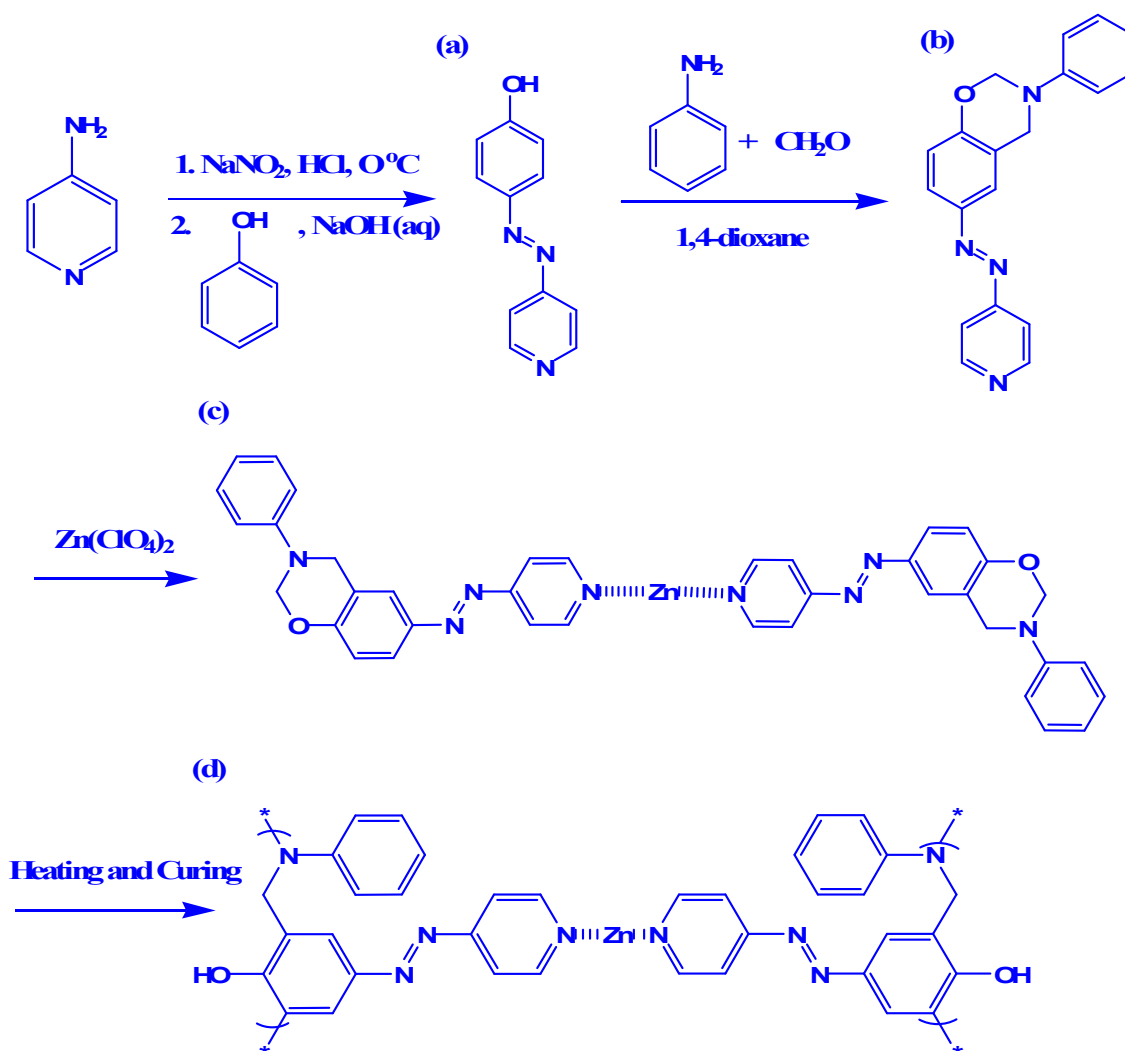
<sup>c</sup>School of Chemical Engineering, East China University of Science and Technology, Shanghai, China

<sup>d</sup>E-mail: kuosw@faculty.nsysu.edu.tw

<sup>e</sup>Department of Materials Science and Engineering, I-Shou University, Kaohsiung, Taiwan

<sup>f</sup>Department of Polymer-Nano Science and Technology, Chonbuk National University, Jeonju, Korea

\*Department of Materials Science and Engineering, National Taiwan University of Science and Technology, Taiwan



**Scheme 1.** (a, b) Syntheses of (a) Azopy-OH and (b) Azopy-BZ. (c) Metal–ligand coordination of Zn(ClO<sub>4</sub>)<sub>2</sub> and Azopy-BZ; (d) Possible structure of Zn(ClO<sub>4</sub>)<sub>2</sub>/poly(Azopy-BZ) complexes.

the production of polymer–metal complexes in the form of insoluble colored precipitates.<sup>41,51</sup> Furthermore, among known photoresponsive molecules, azobenzene derivatives are the most popular for photoswitching applications<sup>52,53</sup> because they can photoisomerize reversibly between their planar trans forms and nonplanar cis form upon irradiation with light. Azobenzene derivatives have two major advantages over other molecules when used as photoswitches: their chemical synthesis is relatively simple (indeed, some are commercially available) and they exhibit chemical stability, allowing repeated trans-to-cis photoisomerizations without decomposition—even under aqueous conditions. In addition, trans-to-cis isomerization occurs with irradiation near 350 nm, while cis-to-trans isomerization is induced by harmless visible light.

In this study we prepared a benzoxazine derivative, Azopy-BZ, featuring an azobenzene/pyridine functional group. First, we prepared 4-(4-hydroxyphenylazo)pyridine (Azopy-OH) through a diazonium reaction of 4-aminopyridine with phenol in the presence of NaOH [Scheme 1(a)]. Next, we obtained Azopy-BZ through the reaction of Azopy-OH, paraformaldehyde, and aniline in 1,4-dioxane [Scheme 1(b)]. We then investigated the physical properties and specific interactions of Azopy-BZ when blended with various weight ratios of zinc perchlorate

[Zn(ClO<sub>4</sub>)<sub>2</sub>] before [Scheme 1(c)] and after [Scheme 1(d)] thermal curing. We employed differential scanning calorimetry (DSC), Fourier transform infrared (FTIR) spectroscopy, dynamic mechanical analysis (DMA), and contact angle analyses to examine the thermal behavior, specific interactions, and surface properties of these materials.

## 35 Experimental Section

### Materials

4-Aminopyridine, paraformaldehyde (96%), sodium nitrite (99%), hydrochloric acid (ca. 37%), aniline (99.8%), EtOAc, tetrahydrofuran, and hexane were purchased from Acros. NaOH and 1,4-dioxane were obtained from Aldrich, as was zinc perchlorate hexahydrate [Zn(ClO<sub>4</sub>)<sub>2</sub>·6H<sub>2</sub>O], which was dried in a vacuum oven at 70 °C for 24 h prior to use.

### Azopy-OH

A solution of phenol (5.0 g, 53 mmol) and sodium nitrite (4.0 g, 58 mmol) in 10% (w/w) aqueous NaOH (20 mL) was added dropwise to a solution of 4-aminopyridine (6.0 g, 64 mmol) in 7.3

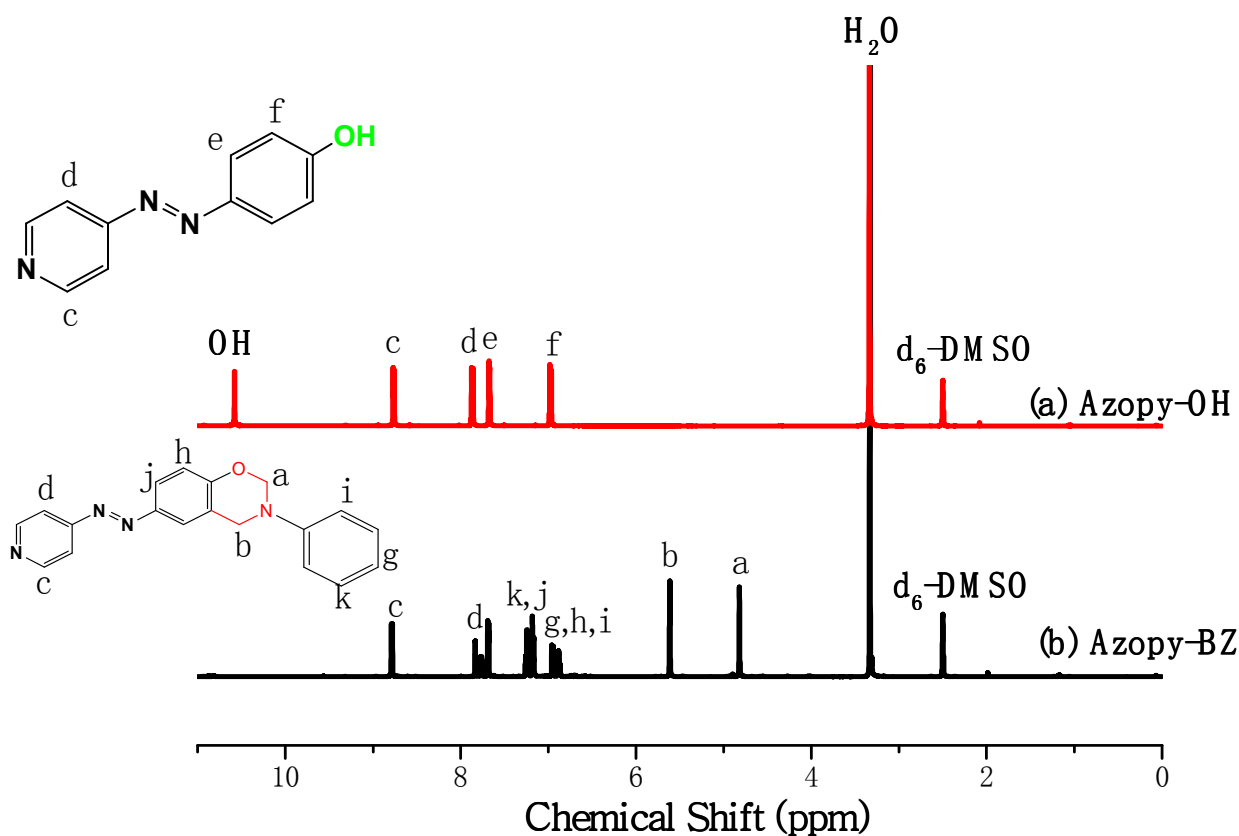


Figure 1.  $^1\text{H}$  NMR spectra of (a) Azopy-OH and (b) Azopy-BZ.

N HCl (45 mL) at 0 °C. The mixture was adjusted to pH 6 through the addition 10% aqueous NaOH. The orange precipitate was filtered off, washed with water, dried and recrystallized (acetone/water) to give the product (3.5 g, 35%). M.p. (DSC): 263–265 °C.  $^1\text{H}$  NMR ( $\delta$ ,  $\text{DMSO}-d_6$ ): 6.98 (d, 2H), 7.67 (d, 2H), 7.88 (d, 2H), 8.77 (d, 2H), 10.59 (s, 1H).  $^{13}\text{C}$  NMR ( $\delta$ ,  $\text{DMSO}-d_6$ ): 162.29, 156.81, 151.32, 145.24, 125.77, 116.18, 115.77. IR (KBr,  $\text{cm}^{-1}$ ): 3204–3463 (OH).

#### Azopy-BZ

A solution of aniline (1.03 g, 11 mmol) in 1,4-dioxane (25 mL) was added portionwise to a solution of paraformaldehyde (0.66 g, 22 mmol) in 1,4-dioxane (100 mL) in a 250-mL flask cooled in an ice bath. The mixture was stirred for 20 min at a temperature below 5 °C and then a solution of Azopy-OH (2.0 g, 10 mmol) in 1,4-dioxane (30 mL) was added. The mixture was heated under reflux at 90–95 °C for 24 h. After cooling, rotary evaporation of the solvent gave a viscous residue that was dissolved in EtOAc (100 mL) and washed several times with 5%  $\text{NaHCO}_3$  and finally with distilled water. The organic phase was dried ( $\text{MgSO}_4$ ), filtered, and concentrated under vacuum to afford an orange residue, which was purified through column chromatography ( $\text{SiO}_2$ ; *n*-hexane/THF, 1:1) to give an orange powder (65%). M.p. (DSC): 163 °C.  $^1\text{H}$  NMR ( $\delta$ ,  $\text{DMSO}-d_6$ ): 4.82 (s, 2H,  $\text{CH}_2\text{N}$ ), 5.61 (s, 2H,  $\text{OCH}_2\text{N}$ ), 6.88 (s, 1H, CH), 6.94 (s, 1H), 6.96 (d, 2H), 7.16 (d, 2H), 7.23 (d, 2H), 7.84 (d, 2H), 8.79 (d, 2H).  $^{13}\text{C}$  NMR ( $\delta$ ,  $\text{DMSO}-d_6$ ): 48.59 ( $\text{CCH}_2\text{N}$ ), 79.79 ( $\text{OCH}_2\text{N}$ ), 115.76–158.32 (aromatic). IR (KBr,  $\text{cm}^{-1}$ ): 1230 (asymmetric C–O–C stretching); 1341 ( $\text{CH}_2$  wagging); 915, 923, and 1490 (trisubstituted benzene ring); 1441 (stretching of trans N=N).

#### Characterization

$^1\text{H}$  and  $^{13}\text{C}$  nuclear magnetic resonance (NMR) spectra were recorded using an INOVA 500 instrument, with DMSO as the solvent and TMS as the external standard. Chemical shifts are reported in parts per million (ppm). FTIR spectra of the polymer films were recorded using a Bruker Tensor 27 FTIR spectrophotometer and the conventional KBr disk method; 32 scans were collected at a spectral resolution of 4  $\text{cm}^{-1}$ . The films tested in this study were sufficiently thin to obey the Beer–Lambert law. FTIR spectra recorded at elevated temperatures were obtained from a cell mounted inside the temperature-controlled compartment of the spectrometer. Dynamic curing kinetics was determined using a TA Q-20 differential scanning calorimeter operated under a  $\text{N}_2$  atmosphere. The sample (ca. 5 mg) was placed in a sealed aluminum sample pan. Dynamic curing scans were recorded from 30 to 350 °C at a heating rate of 20 °C  $\text{min}^{-1}$ . The thermal stability of the samples was measured using a TG Q-50 thermogravimetric analyzer operated under a  $\text{N}_2$  atmosphere. The cured sample (ca. 5 mg) was placed in a Pt cell and heated at a rate of 20 °C  $\text{min}^{-1}$  from 30 to 800 °C under a  $\text{N}_2$  flow rate of 60  $\text{mL min}^{-1}$ . DMA was performed using a PerkinElmer instruments DMA 8000 apparatus operated in tension mode and the preparation of the samples for DMA; the sample powder was sandwiched in the middle of a single cantilever and the bending was measured at temperatures from room temperature to 250 °C. Analyses of the loss tangent ( $\tan \delta$ ) were recorded automatically by the system; the heating rate and frequency were fixed at 2 °C  $\text{min}^{-1}$  and 1 Hz, respectively. UV–Vis spectra were recorded using a Shimadzu mini 1240 spectrophotometer. Photoisomerization of the azobenzene unit was performed using a UV–Vis lamp directly at 365 nm (UV, 90

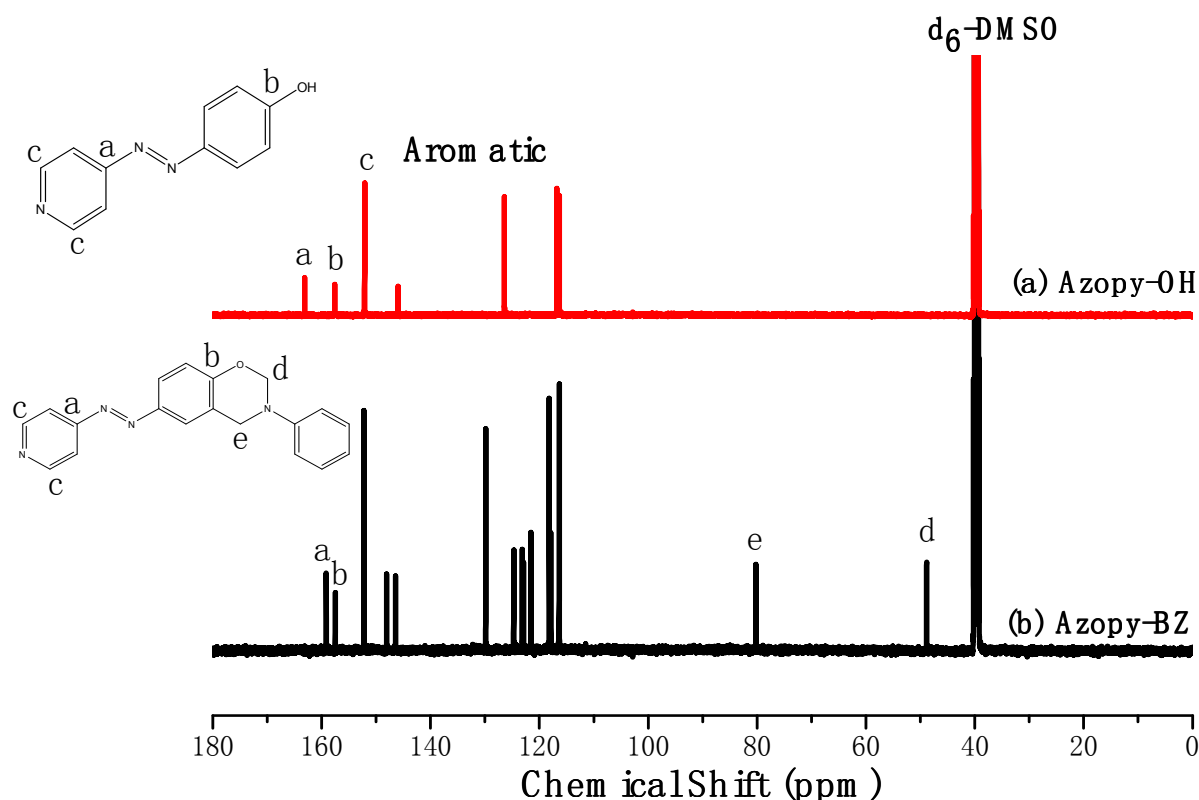


Figure 2.  $^{13}\text{C}$  NMR spectra of (a) Azopy-OH and (b) Azopy-BZ.

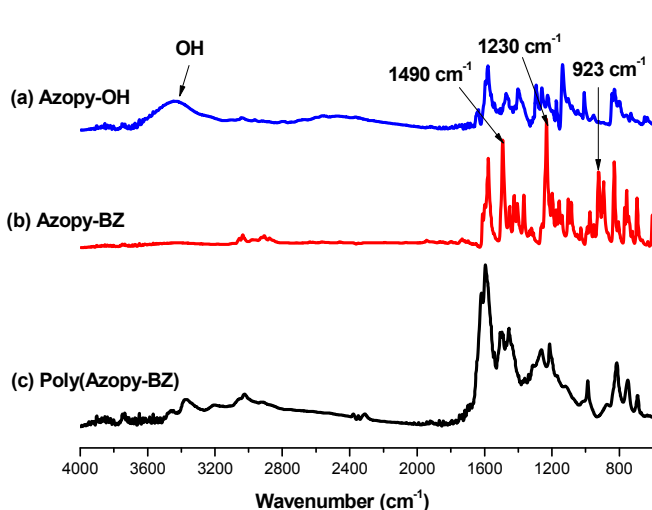


Figure 3. FTIR spectra of (a) Azopy-OH, (b) Azopy-BZ, and (c) Poly(Azopy-BZ), recorded at room temperature.

mW  $\text{cm}^{-2}$ ) and through a filter at 400–500 nm (visible, 90 mW  $\text{cm}^{-2}$ ) to generate the light for the trans-to-cis and cis-to-trans isomerizations, respectively. The concentration of Azopy-BZ in THF was  $10^{-4}$  M for the UV-Vis spectroscopic study. The contact angles of the polymer samples before and after curing were measured at 25 °C using a FDSA Magic Droplet100 contact angle goniometer interfaced with image capture software after injecting a 5- $\mu\text{L}$  liquid drop. To obtain reliable contact data, at least three droplets were measured at different regions of the same piece of film, with at least two pieces of film being used.

Thus, at least six advancing contact angles were averaged for each type of film with each type of solvent. Deionized water was used as a standard when measuring the surface properties.

## 25 Results and Discussion

### Synthesis of Azopy-BZ Through Mannich Reaction of Azopy-OH With Aniline and Paraformaldehyde

We prepared Azopy-BZ in high purity and high yield, even though it was possible that we might generate various side products, due to the high reactivity of pyridyl and its ability to form hydrogen bond intramolecularly with phenolic groups. Figure 1 presents the  $^1\text{H}$  NMR spectra of Azopy-OH and Azopy-BZ. The spectrum of Azopy-OH [Figure 1(a)] features a signal at 10.58 ppm corresponding to the proton of the phenolic OH group, with the signals of the aromatic protons of the azobenzene pyridine unit appearing as multiplets in the range 6.97–8.77 ppm. The spectrum of Azopy-BZ [Figure 1(b)] features the signals for the  $\text{CH}_2\text{N}$  and  $\text{OCH}_2\text{N}$  bridges of the oxazine unit at 4.82 and 5.61 ppm, respectively. The signal of the proton of the phenolic OH group of Azopy-OH is absent, but the signals of the azobenzene pyridine moiety are present, confirming the successful synthesis of Azopy-BZ.

Figure 2 presents the  $^{13}\text{C}$  NMR spectra of Azopy-OH and Azopy-BZ. The signals of the azobenzene pyridine moiety appear in the range from 115.75 to 158.32 ppm in Figure 2(a). Two peaks appear at 48.6 and 79.9 ppm in the spectrum of Azopy-BZ in Figure 2(b), representing the carbon nuclei of the oxazine ring; the signals of the azobenzene pyridine ring confirm the successful synthesis of Azopy-BZ. Figure 3 presents the FTIR spectra of Azopy-OH and Azopy-BZ at room temperature and of poly(Azopy-BZ) after thermal curing. The spectrum of Azopy-OH features a sharp signal for the OH group at 3442  $\text{cm}^{-1}$  and



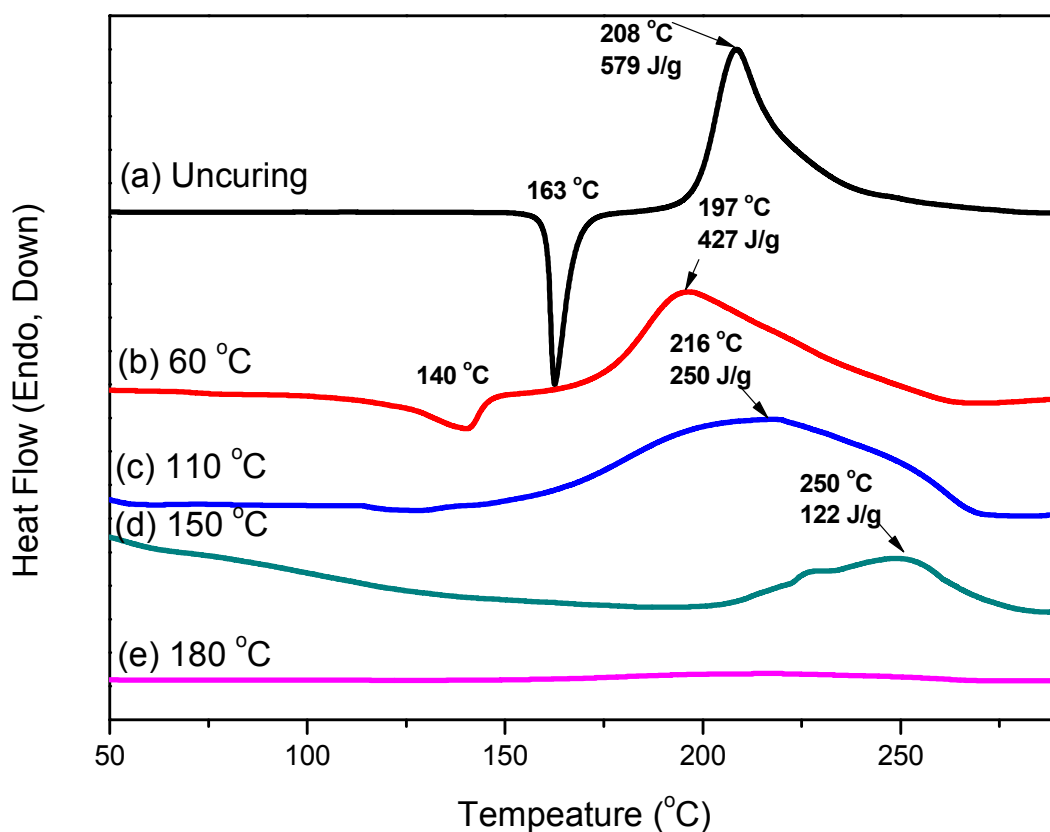


**Figure 4.** DSC thermograms of Azopy-BZ, recorded after each curing stage.

absorption bands for the aromatic ring at 3025, 1610, and 1571  $\text{cm}^{-1}$  [Fig. 3(a)]. In the spectrum of Azopy-BZ [Fig. 3(b)], the signal for the phenolic OH group is absent, but signals are evident for C–C stretching vibrations of the 1,2,4-substituted benzene ring at 1490 and 923  $\text{cm}^{-1}$  for the oxazine ring, for asymmetric C–O–C stretching at 1229  $\text{cm}^{-1}$ , and for stretching of the trans N=N bond at 1440  $\text{cm}^{-1}$ . Together, these spectroscopic features confirmed the successful synthesis of Azopy-BZ. Figure 3(c) presents the FTIR spectrum recorded after thermal curing of pure Azopy-BZ. The characteristic absorption bands at 1490 and 923  $\text{cm}^{-1}$  for the trisubstituted aromatic ring of Azopy-BZ disappeared after thermal curing, with the former shifting to 1502  $\text{cm}^{-1}$  for the tetrasubstituted aromatic ring of poly(Azopy-BZ). The broad absorption bands in the range 2600–3500  $\text{cm}^{-1}$  in Fig. 3(c) represent three different kinds of hydrogen bonding interactions: intramolecular [O $\cdots$ H–N $^+$ ] hydrogen bonding (ca. 2800  $\text{cm}^{-1}$ ), intramolecular [O–H $\cdots$ N] hydrogen bonding (ca. 3200  $\text{cm}^{-1}$ ), and intermolecular [O–H $\cdots$ O] hydrogen bonding (ca. 3342  $\text{cm}^{-1}$ ); the identities of these signals have been reported previously.<sup>18,54</sup>

#### 25 Thermal Polymerization of Azopy-BZ

We used DSC to determine the curing behavior of pure Azopy-BZ (Figure 4). The DSC trace of uncured Azopy-BZ featured a sharp melting peak at 163 °C, revealing the high purity of our Azopy-BZ monomer. A sharp exothermic peak, which we attribute to the ring opening polymerization of Azopy-BZ, appeared with its onset at 198 °C and its maximum at 208 °C; it had a reaction heat of 579 J g $^{-1}$ . The curing temperature for

Azopy-BZ (208 °C) shifted from 263 °C for conventional 3-phenyl-3,4-dihydro-2H-benzoxazine (Pa-type),<sup>1</sup> presumably because of the basicity of the azo and pyridyl groups, suggesting that the azobenzene and pyridine moieties acted as basic catalysts that contributed to the lower polymerization temperature. After thermal curing of pure Azopy-BZ at 110 °C, the first melting peak was absent from the DSC curve, with the intensity of the exotherm decreasing upon increasing the curing temperature, almost disappearing after thermal curing at temperatures between 150 and 180 °C. Figure 5 displays FTIR spectra of Azopy-BZ after various curing stages. Upon increasing the curing temperature, we observed a decrease in the intensities of the characteristic absorption bands of the benzoxazine unit at 923  $\text{cm}^{-1}$  (C–O–C symmetric), 1230  $\text{cm}^{-1}$  (C–O–C asymmetric), and 1490  $\text{cm}^{-1}$ .<sup>1</sup> After curing at 180 °C, these characteristic absorption bands had disappeared completely, suggesting that ring opening of the benzoxazine units had reached completion. In addition, after curing 150 °C, we observed a new absorption band at 2800–3400  $\text{cm}^{-1}$ , consistent with the formation of a phenolic OH group. These features are consistent with the progress of the ring opening polymerization of Azopy-BZ during thermal curing. Figure 6 displays TGA thermograms of pure Azopy-BZ before and after thermal curing at 60, 110, 150, and 180 °C under N $_2$ . The thermal stability, the decomposition temperature (10 wt% loss), and the char yield all decreased after curing at 60 and 110 °C, presumably because of loss of the crystal structure at these curing temperatures, consistent with the DSC traces in Figure 4. Further increases in the curing temperature to 150 and 180 °C caused the decomposition temperature and char yield to increase,

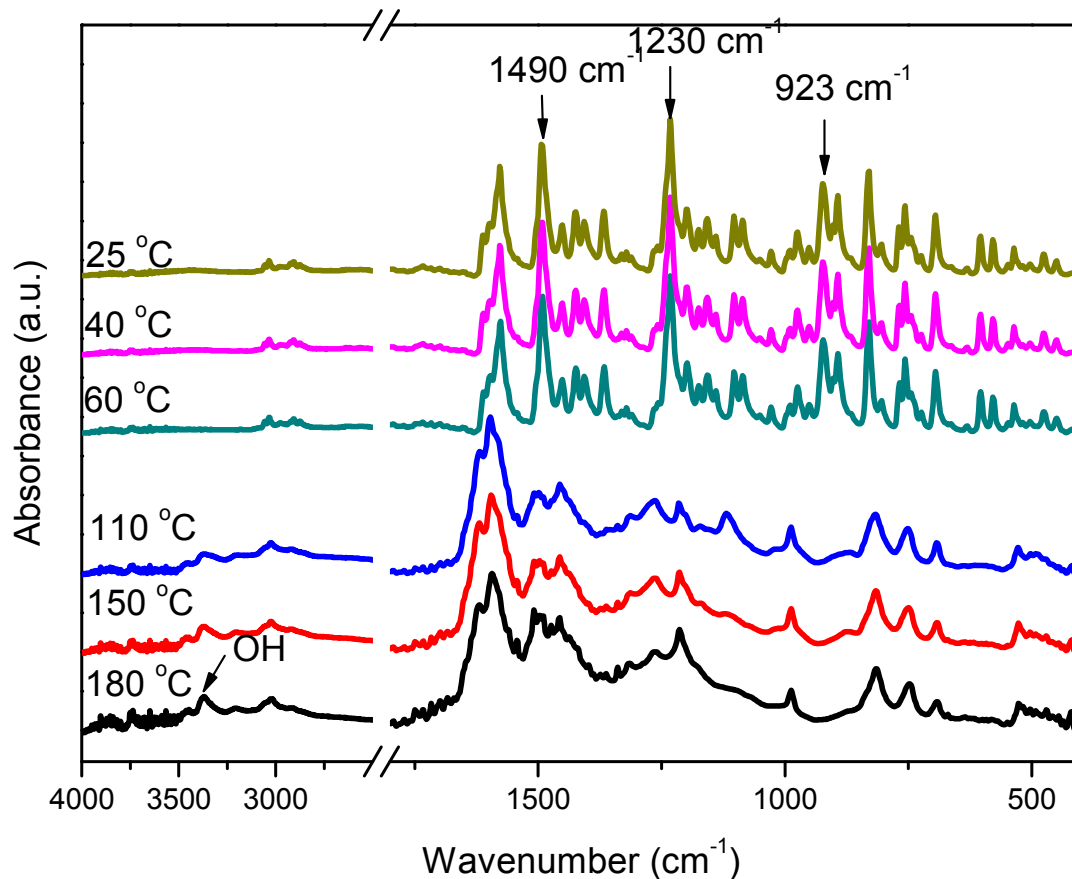


Figure 5. FTIR spectra of Azopy-BZ, recorded after each curing stage.

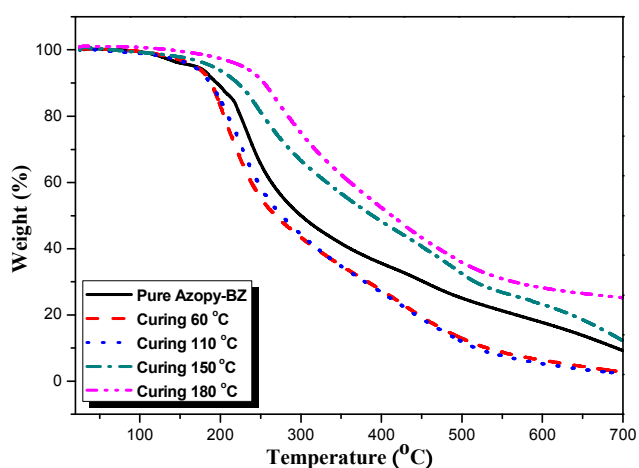


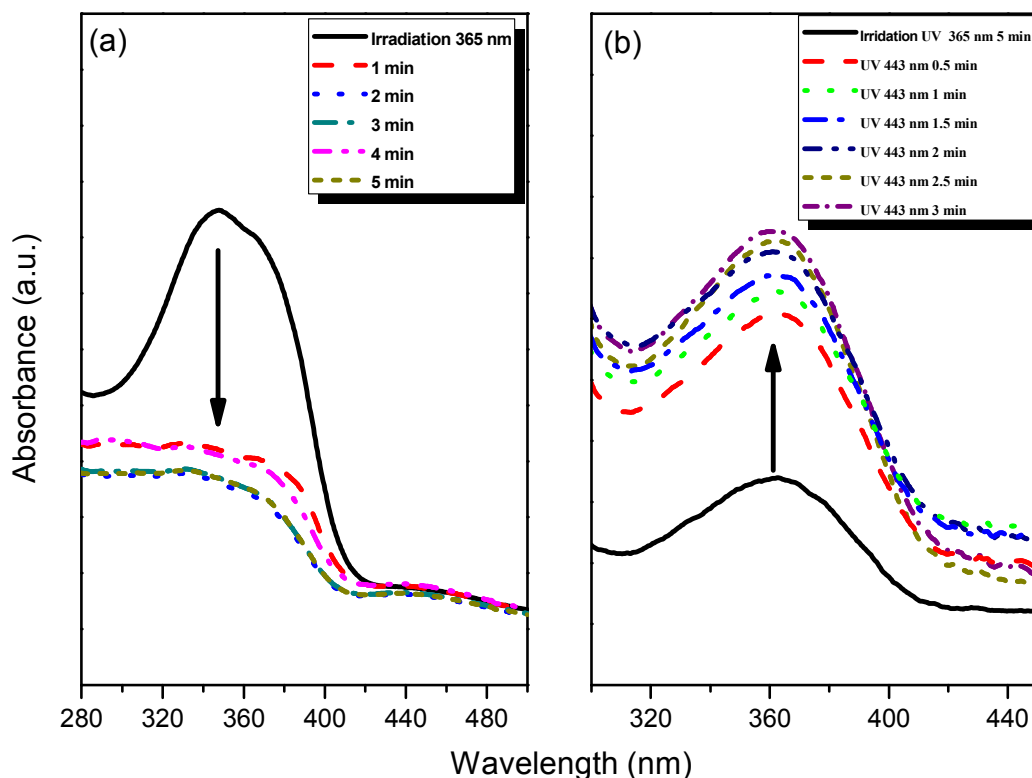
Figure 6. TGA analyses of Azopy-BZ, recorded after each curing stage.

consistent with increased crosslinking densities enhancing the thermal stabilities of the resulting poly(Azopy-BZ) species.

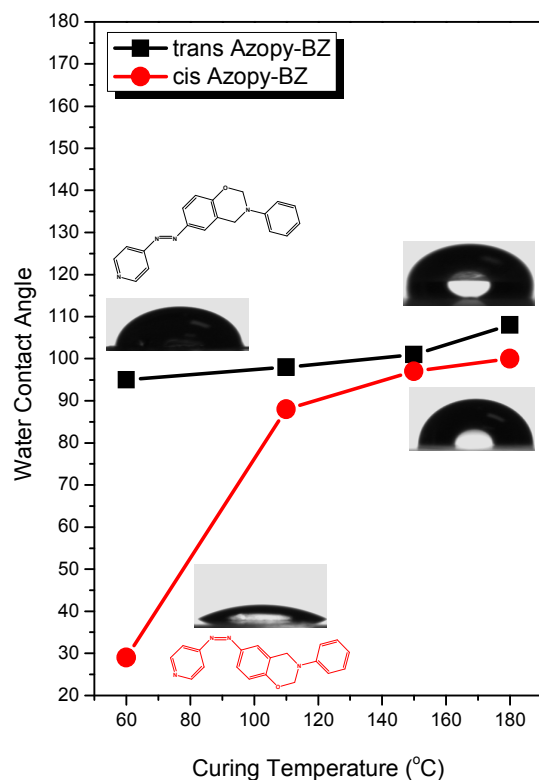
#### Photoisomerization of Azopyridine Chromophore in Azopy-BZ

Figure 7 presents UV-Vis absorption spectra revealing the photoisomerization of the azopyridine chromophore in Azopy-BZ. Figure 7(a) displays the change in the UV-Vis absorption

spectra of the Azopy-BZ solution upon irradiation with UV light at 365 nm. The maximum absorption at 360 nm was due to the  $\pi$ - $\pi^*$  transition of the *trans*-azopyridine group. Upon irradiation with UV light, the intensity of the absorbance at 360 nm decreased gradually, eventually reaching a relatively stable value. At the same time, the intensity of the signal near 333 nm, which we assign to the  $\pi$ - $\pi^*$  transition of the *cis* isomer increased. Eventually, the wavelength of maximum absorption shifted from 360 to 333 nm. These variations are consistent with the *trans*-to-*cis* isomerization of the azopyridine group in Azopy-BZ. Figure 7(b) reveals the change in the UV-Vis absorption spectra of the Azopy-BZ solution upon irradiation with UV light at 443 nm; the intensity of the absorbance at 360 nm increased gradually until reaching a stable state after 3 min, consistent with *cis*-to-*trans* isomerization of the azopyridine group. Figure 8 displays the contact angles of water for pure Azopy-BZ before and after its photoisomerization under a UV lamp at 365 nm, as well as after thermal curing at 60, 110, and 150 °C for 3 h and at 180 °C for 2 h. The water contact angles of Azopy-BZ at room temperature and after thermal curing at 60, 110, and 150 °C were 89, 95, 98, and 101°, respectively; after thermal curing at 180 °C, it reached 108°. Notably, after *trans*-to-*cis* photoisomerization of Azopy-BZ at 60, 110, 150 and 180 °C, the water contact angles changed completely to 29, 88, 97, and 100°, respectively. The water contact angle of the *trans* isomer of Azopy-BZ (95°) was larger than that of the *cis* isomer of Azopy-BZ (29°) after curing at 60 °C; this behavior is consistent with the *trans* isomer having a smaller dipole moment and lower surface free energy (and,



**Figure 7.** UV-Vis absorption spectra of Azopy-BZ ( $10^{-4}$  M in THF) (a) before and (b) after irradiation with UV light at 365 nm for different periods of time.



**Figure 8.** Water contact angles of Azopy-BZ in its trans and cis isomeric forms, recorded after each curing stage.

therefore, a higher water contact angle) and the cis form possessing a bigger dipole moment and higher surface free energy (and, therefore, a lower water contact angle).<sup>55</sup> The water contact angles increased upon increasing the thermal curing temperature and time for both the trans and cis isomers, due to increased degrees of intramolecular hydrogen bonding and lower surface free energies after thermal curing of the benzoxazine monomer. FTIR spectra revealed (Figure 5) that four different types of hydrogen bonds were present upon increasing the curing temperature: intramolecular  $[O^{\cdot\cdot}H^+N]$  hydrogen bonds ( $2830\text{ cm}^{-1}$ ), intramolecular  $[OH^{\cdot\cdot}N]$  (from Mannich bridge) hydrogen bonds ( $3200\text{ cm}^{-1}$ ), intermolecular  $[OH^{\cdot\cdot}O]$  and  $[OH^{\cdot\cdot}N]$  (from pyridyl) hydrogen bonds ( $3400\text{--}3370\text{ cm}^{-1}$ ), and intramolecular  $[OH^{\cdot\cdot}\pi]$  hydrogen bonds ( $3459\text{ cm}^{-1}$ ), as have been noted in previous reports.<sup>18,54</sup> As a result, the strong intramolecular  $[OH^{\cdot\cdot}N]$  hydrogen bonds (from the Mannich bridge) dominated for low surface free energy than photoisomer of Azopy-BZ monomer, but we also found that the water contact angle of the trans isomer remained larger than that of the cis isomer after thermal curing.

#### Thermal Polymerization of Azopy-BZ Blended With $Zn(ClO_4)_2$

We used DSC to investigate the thermal curing behavior of pure Azopy-BZ in the presence of various amounts of  $Zn(ClO_4)_2$  (Figure 9). The melting peak disappeared after blending with this zinc salt, indicating that the crystal structure was destroyed upon the interactions of the  $Zn^{2+}$  ions with the pyridine or azo groups. Interestingly, prior to thermal curing of the samples containing 1 or 2 wt% of  $Zn(ClO_4)_2$ , we observed three major curing peaks: near 130, 190, and 233 °C, respectively. The first two curing peaks presumably arose from ring opening of the benzoxazine



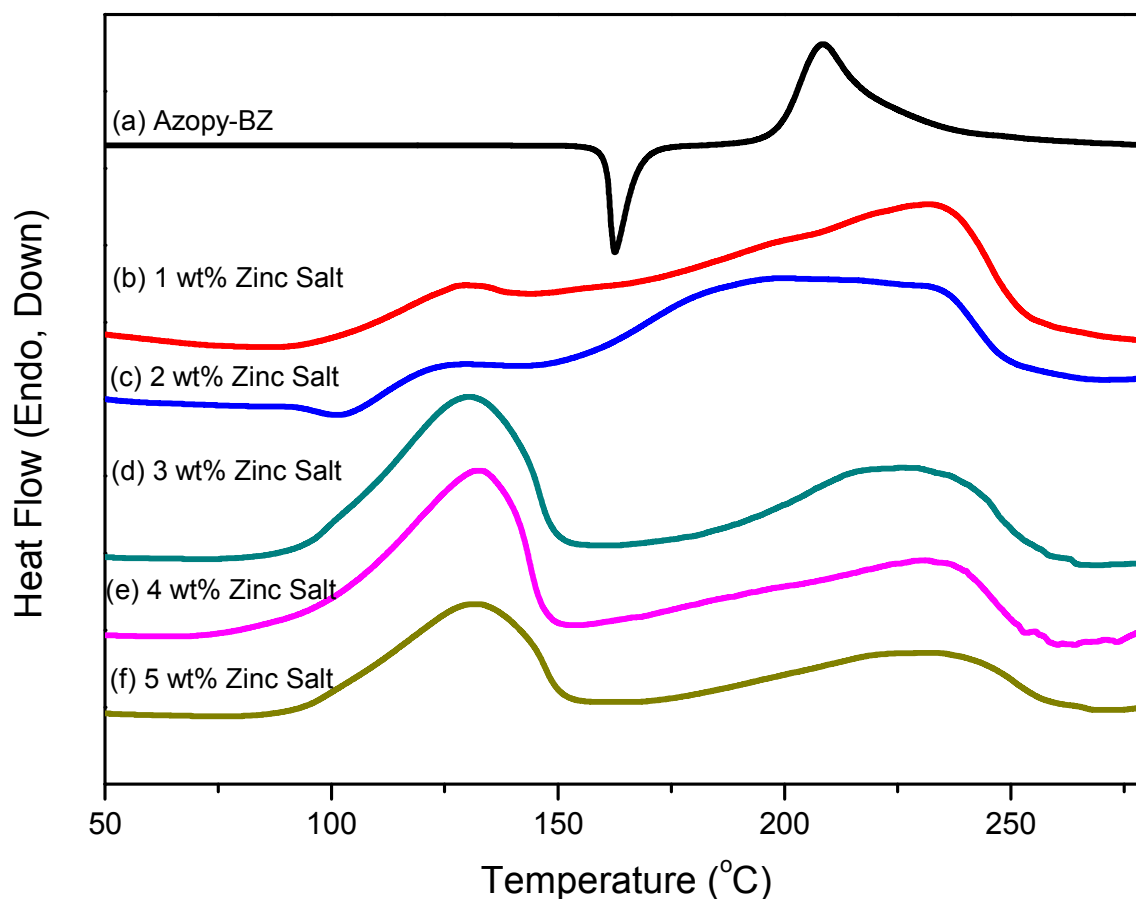
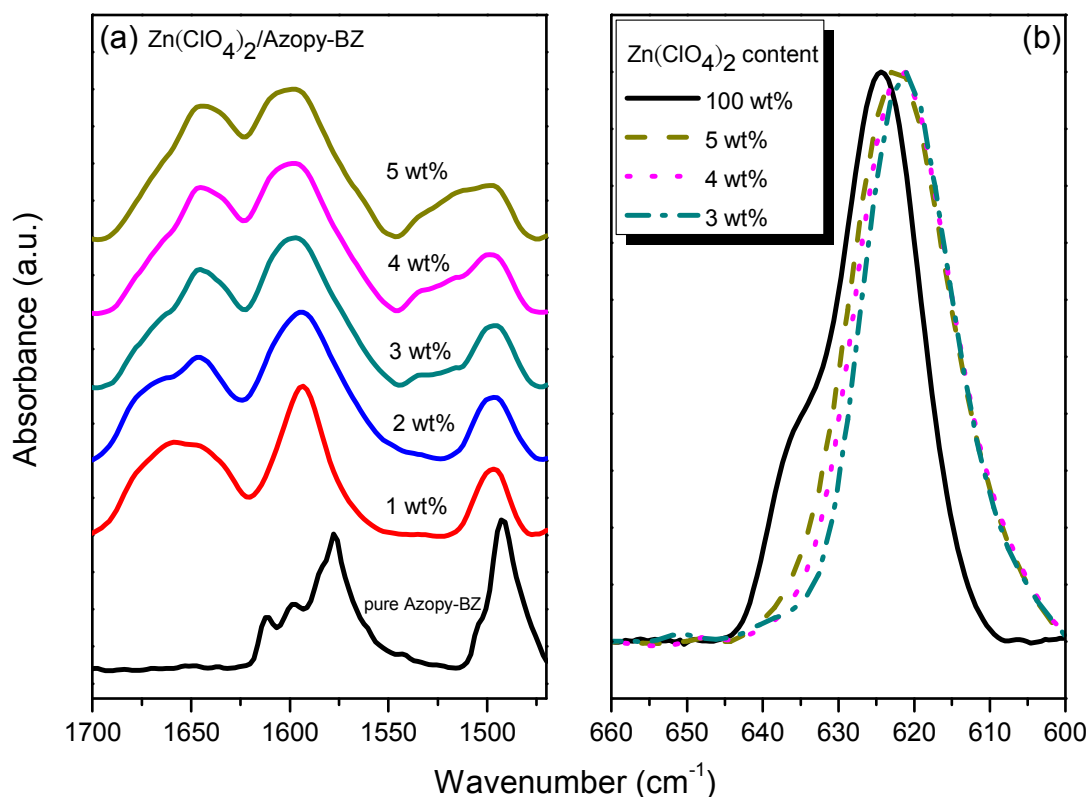


**Figure 9.** DSC thermograms of Azopy-BZ in the presence of various amounts of  $\text{Zn}(\text{ClO}_4)_2$ .

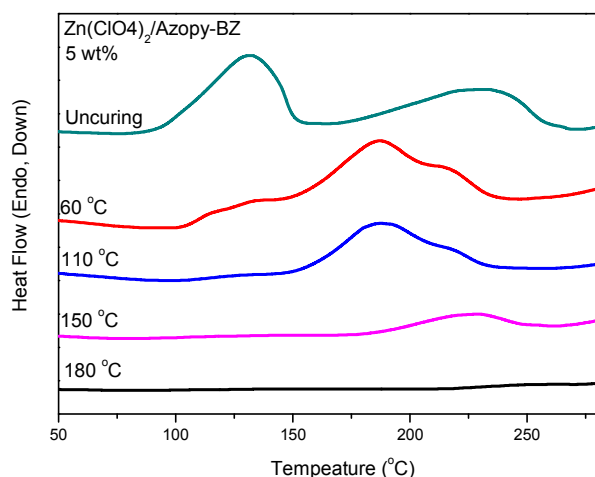
units coordinated with  $\text{Zn}^{2+}$  ions, while the latter corresponds to the curing of the non-coordinated benzoxazine units. The curing peak shifted to lower temperature upon the addition of  $\text{Zn}(\text{ClO}_4)_2$ , indicating that the  $\text{Zn}^{2+}$  ions could initiate the ring opening process.<sup>56,57</sup> Ishida et al. reported that transition metal salts initiate ring opening, but not the polymerization of Ba-type benzoxazine.<sup>56</sup> The temperature for ring opening of the benzoxazine units shifted from 208 °C in the absence of  $\text{Zn}(\text{ClO}_4)_2$  to 233 °C in its presence because the initial ring opening in the presence of  $\text{Zn}(\text{ClO}_4)_2$  resulted in a certain degree of crosslinking that inhibited the purely thermal curing of the remaining benzoxazine groups. Further increasing the  $\text{Zn}(\text{ClO}_4)_2$  content to 3–5 wt% caused the second peak at 190 °C to shift completely to 130 °C, thereby increasing the enthalpy of curing at the first peak. Notably, the intensity of the curing peak at 233 °C did not change accordingly, and the total enthalpy of curing of the overall reaction remained relatively unchanged.

Figure 10(a) presents FTIR spectra of Azopy-BZ blended with various weight ratios of  $\text{Zn}(\text{ClO}_4)_2$  prior to thermal curing. Signals for the stretching of the pyridine ring appeared at 1598, 1490, and 993  $\text{cm}^{-1}$ , with these peaks sometimes overlapping with those representing the aromatic ring; indeed, we observed three major peaks at 1612, 1598, and 1576  $\text{cm}^{-1}$  for aromatic stretching of the C=C bonds in the phenyl-O-C, pyridine ring, and phenyl-N-C groups of Azopy-BZ. Upon addition of  $\text{Zn}(\text{ClO}_4)_2$ , a new band appeared at 1644  $\text{cm}^{-1}$ , the fraction of which increased

upon increasing the content of the salt. In a previous study of  $\text{Zn}(\text{ClO}_4)_2/\text{P4VP}$  blend systems, we found that, upon addition of  $\text{Zn}(\text{ClO}_4)_2$ , a similar new band appeared at a relatively high wavenumber; we assigned this signal as resulting from the  $\text{Zn}^{2+}$  coordinating to pyridine rings.<sup>58</sup> Pires et al. reported that the pyridine units in P4VP behave as  $\pi$ -bonding ligands when coordinated to this cation.<sup>59</sup> Therefore, the higher energy of this new absorption band is the result of the formation of such a coordination complex. Ishida et al. found, however, that treatment of benzoxazines with metal salts resulted in an increase in the content of OH groups, indicating the presence of ring-opened structures. They also detected a band at 1654  $\text{cm}^{-1}$  after blending with metal salts, tentatively assigned to conjugated C=O groups, possibly quinone-like structures. The OH groups of phenols can be oxidized by metal ions to form quinone structures.<sup>56</sup> The structure of Azopy-BZ, however, differs from that of a Ba-type benzoxazine in that it possesses another pyridyl group, which could also interact with  $\text{Zn}(\text{ClO}_4)_2$ . To confirm whether such an interaction existed, Figure 10(b) displays the region of the FTIR spectra featuring the stretching bands of  $\text{ClO}_4^-$  (from 660 to 600  $\text{cm}^{-1}$ ) for pure  $\text{Zn}(\text{ClO}_4)_2$  and for various  $\text{Zn}(\text{ClO}_4)_2/\text{Azopy-BZ}$  blends. In this region, absorptions at 627 and 635  $\text{cm}^{-1}$  represent vibrations of the free and contacted  $\text{ClO}_4^-$  ions, respectively.<sup>60</sup> When the concentration of  $\text{Zn}(\text{ClO}_4)_2$  decreased, the band for the contacted ion shifted to lower frequency and became symmetric. We attribute the asymmetric shape of the band for pure  $\text{Zn}(\text{ClO}_4)_2$



**Figure 10.** FTIR spectra of Azopy-BZ in the presence of various amounts of  $\text{Zn}(\text{ClO}_4)_2$ , recorded at room temperature.



**Figure 11.** DSC thermograms of Azopy-BZ in the presence of 5 wt%  $\text{Zn}(\text{ClO}_4)_2$ , recorded after each curing stage.

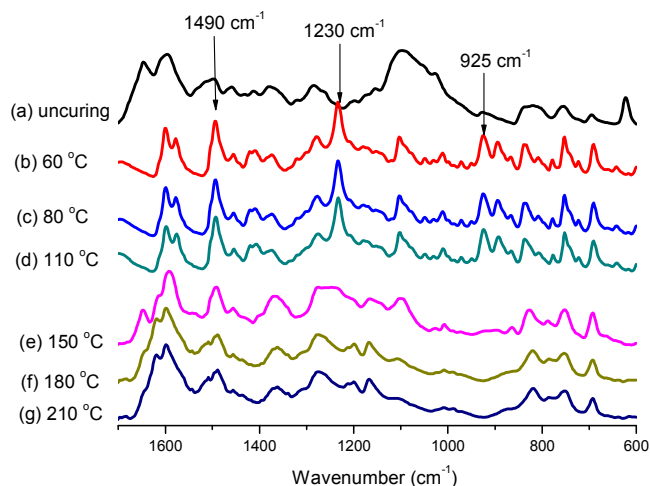
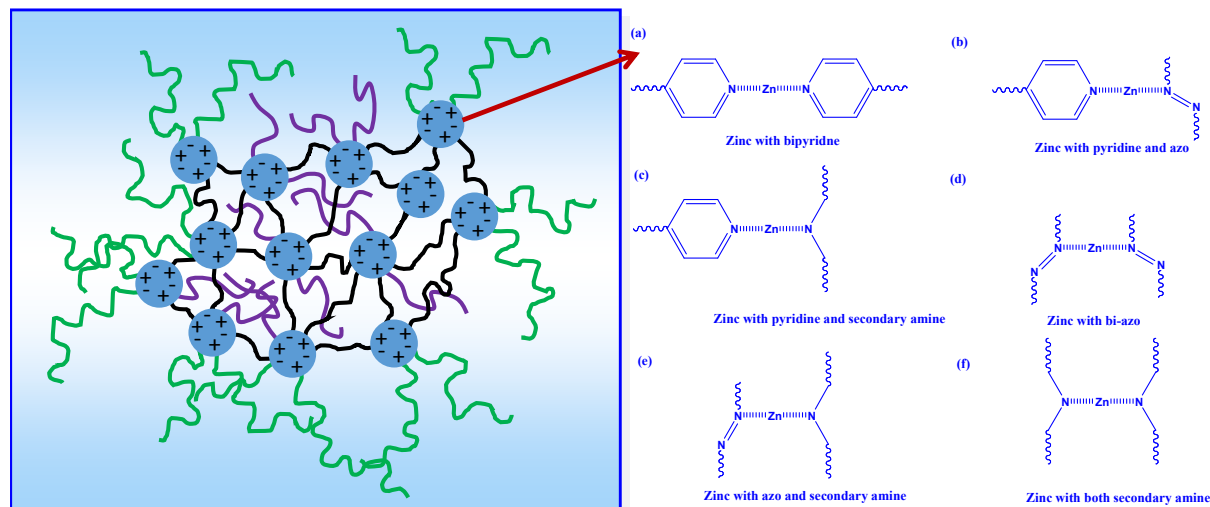


**Figure 12.** FTIR spectra of Azopy-BZ in the presence of 5 wt%  $\text{Zn}(\text{ClO}_4)_2$ , recorded after each curing stage.

to the existence of both free ions and ion pairs. Blending with Azopy-BZ caused the fraction of contacted ions to decrease, consistent with the  $\text{Zn}^{2+}$  ion interacting with the pyridyl group of Azopy-BZ, causing the fraction of free  $\text{ClO}_4^-$  anions to increase. We found that the degree of coordination of the pyridine rings increased upon increasing the content of  $\text{Zn}(\text{ClO}_4)_2$ .

Figure 11 presents the thermal curing behavior of Azopy-BZ containing 5 wt%  $\text{Zn}(\text{ClO}_4)_2$ . As mentioned above, two major curing peaks appeared at 130 and 233 °C, corresponding to ring opening of the  $\text{Zn}^{2+}$ -coordinated benzoxazine units and to the original curing of benzoxazine units, respectively. After thermal curing at 60 °C, the intensity of the first exotherm peak decreased, eventually disappearing after thermal curing at 110 °C. The first curing peak shifted to 190 °C, the same curing temperature as that



Scheme 2: (Left) Possible morphology of a  $\text{Zn}(\text{ClO}_4)_2/\text{poly}(\text{Azopy-BZ})$  complex. (Right) Possible modes of metal–ligand coordination between  $\text{Zn}(\text{ClO}_4)_2$  and  $\text{poly}(\text{Azopy-BZ})$ .

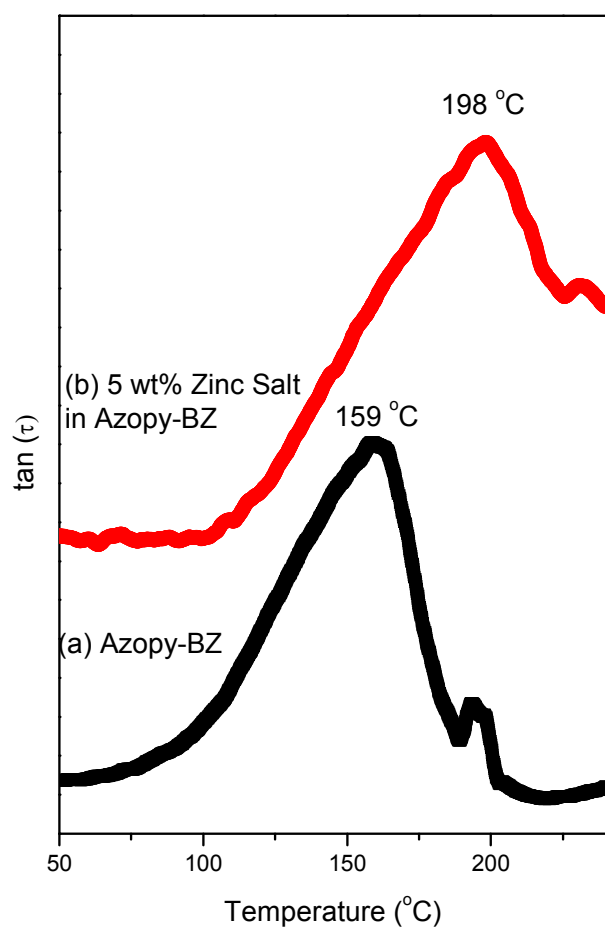


Figure 13. DMA analyses of (a) pure  $\text{poly}(\text{Azopy-BZ})$  and (b)  $\text{Zn}(\text{ClO}_4)_2/\text{poly}(\text{Azopy-BZ}) = 5/95$  after thermal curing.

for the second peak of the non-cured Azopy-BZ after blending with 1 wt%  $\text{Zn}(\text{ClO}_4)_2$  (see Figure 9). After thermal curing at 150 °C, this curing peak also disappeared and shifted to 228 °C, corresponding to the temperature of thermal curing of the original benzoxazine. After thermal curing at 180 °C, the exotherm peaks disappeared completely, suggesting that the ring opening polymerization of Azopy-BZ was complete in the presence of 5 wt%  $\text{Zn}(\text{ClO}_4)_2$ .

Figure 12 presents FTIR spectra of Azopy-BZ blended with 5 wt%  $\text{Zn}(\text{ClO}_4)_2$  after thermal curing at various temperatures. After thermal curing at 60 °C, the absorption peaks at 1640 and 1092  $\text{cm}^{-1}$  disappeared, presumably because of dissociation of the  $\text{Zn}^{2+}$  ions coordinated with the pyridyl units. After thermal curing at 150 and 180 °C, the characteristic absorption bands of the trisubstituted aromatic rings of the oxazine units at 1490 and 925  $\text{cm}^{-1}$  disappeared, with signals for the phenolic OH groups, arising from ring opening, appearing at 1630 and 1512  $\text{cm}^{-1}$ . Liu et al. reported that the metal salts perform three major steps during the ring opening of benzoxazine. First, the catalyst coordinates with the oxygen and nitrogen atoms of the oxazine ring; then, subsequent electrophilic reactions involve O attack, N attack, and aryl attack; finally, rearrangement occurs from a phenoxy structure to a phenolic structure.<sup>61</sup> We conclude that the  $\text{Zn}^{2+}$  ions effectively coordinated with the oxygen and/or nitrogen atoms during ring opening of the benzoxazine units. In addition, the azopyridine units in Azopy-BZ provided another coordination site to increase the physical crosslinking density, thereby improving the thermal properties after thermal curing.

Finally, we used DMA to investigate the glass transition temperatures of these species. Figure 13 indicates that the glass transition temperature of  $\text{poly}(\text{Azopy-BZ})$  increased from 159 to 198 °C after blending with 5 wt%  $\text{Zn}(\text{ClO}_4)_2$  and thermally curing at 180 °C. The minor peaks at higher temperature may come from another thermal transition for  $\text{poly}(\text{Azopy-BZ})$  matrix. Clearly, The ionic interactions or ionic cluster formation of ionomers usually resemble physical cross-linking.<sup>58,60,62</sup> The mobility of polymer chains was restricted by such physical cross-links, thereby resulting in higher glass transition temperatures than that of the mother polymer, due to increased the ion–polymer and ion–ion interactions of the polybenzoxazine. Scheme 2 displays

some possible modes of metal–ligand coordination in the complex formed between Zn(ClO<sub>4</sub>)<sub>2</sub> and Azopy-BZ.

### Conclusions

We synthesized an azo/pyridine-functionalized polybenzoxazine. DSC revealed that the exothermic peak for the ring opening polymerization of benzoxazine itself shifted to lower temperature because the azo and pyridyl groups acted as basic catalysts for the ring opening process. In addition, the azobenzene group also allowed photoisomerization between its planar trans form and its nonplanar cis form upon irradiation with light, thereby allowing tuning of the surface properties. Furthermore, the azopyridyl moiety in the benzoxazine exhibited high affinity toward Zn<sup>2+</sup> ions, not only promoting the ring opening polymerization to occur at a relatively low curing temperature (only 130 °C) but also leading to the formation of corresponding polymer–metal complexes and, thereby, improving the thermal properties, based on DMA analyses. Because of such metal–ligand bonding, we suspect that such polymers would be useful as metal scavenging materials and as components within polymer/inorganic hybrid materials.

### Acknowledgment

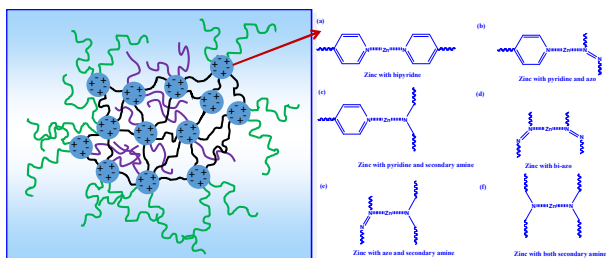
This study was supported financially by the National Science Council, Taiwan, Republic of China, under contracts MOST103-2221-E-110-079-MY3 and MOST102-2221-E-110-008-MY3.

### References

- H. Ishida, “*Handbook of Polybenzoxazine*”, Ishida, H.; Agag, T. Eds., Elsevier, Amsterdam **2011**, Chapter 1, 1.
- Li, X.; Gu, Y. *Polym. Chem.* **2011**, *2*, 2778-2781.
- Ishida, H.; Allen, D. J. *J. Polym. Sci. Part B: Polym. Phys.* **1996**, *34*, 1019-1030.
- Takeichi, T.; Kawachi, T.; Agag, T. *Polym. J.* **2008**, *40*, 1121-1131.
- Ghosh, N. N.; Kiskan, B.; Yagci, Y. *Prog. Polym. Sci.* **2007**, *32*, 1344-1391.
- Nair, C. P. R. *Prog. Polym. Sci.* **2004**, *29*, 401-498.
- Burke, J. W. *J. Am. Chem. Soc.* **1949**, *71*, 609-612.
- Agag, T.; Takeichi, T. *Macromolecules.* **2003**, *36*, 6010-6017.
- Oie, H.; A. Saudo, A.; Endo, T. *J. Polym. Sci. Part A: Polym. Chem.* **2010**, *48*, 5357-5363.
- Ergin, M.; Kiskan, B.; Gacal, B.; Yagci, Y. *Macromolecules.* **2007**, *40*, 4724-4727.
- Nagai, A.; Kamei, Y.; Wang, S.; Omura, M.; Suda, A.; Nishida, H.; Kawamoto, E.; Endo, T. *J. Polym. Sci. Part A: Polym. Chem.* **2008**, *46*, 2316-2325.
- Kiskan, B.; Demirary, G.; Yagci, Y. *J. Polym. Sci. Part A: Polym. Chem.* **2008**, *46*, 3512-3518.
- Chernykh, A.; Agag, T.; Ishida, H.; *Polymer.* **2009**, *50*, 3153-3157.
- Liu, Y. L.; Chou, C. I. *J. Polym. Sci. Part A: Polym. Chem.* **2005**, *43*, 5267-5282.
- Andreu, R.; Espinosa, M. A.; Galia, M.; Cadiz, V.; Ronda, J. C.; A. J. Reina, J. A. *J. Polym. Sci. Part A: Polym. Chem.* **2006**, *44*, 1529-1540.
- Kudoh, R.; Sudo, A.; Endo, T. *Macromolecules.* **2010**, *43*, 1185-1187.
- Kiskan, B.; Koz, Y.; Yagci, Y. *J. Polym. Sci. Part A: Polym. Chem.* **2009**, *47*, 6955-6961.
- Wang, F. C.; Su, C. Y.; Kuo, W. S.; Huang, F. C.; Y Sheen, C. Y.; Chang, C. F. *Angew. Chem. Int. Ed.* **2006**, *45*, 2248-2251.
- Kuo, W. S.; Wu, C. Y.; Wang, F. C.; Jeong, U. K. *J. Phys. Chem. C.* **2009**, *113*, 20666-20673.
- Qu, L.; Xin, Z. *Langmuir.* **2011**, *27*, 8365-8370.
- Wang, F. C.; Chang, C. F.; Kuo, W. S. “*Handbook of Polybenzoxazine*”, Ishida, H.; Agag, T. Eds., Elsevier, Amsterdam **2011**, Chapter 33, 579.
- Lin, H. C.; Chang, L. S.; Shen, Y. T.; Shih, S. Y.; Lin, T. H.; Wang, F. C. *Polym. Chem.* **2012**, *3*, 935-945.
- Wu, C. Y.; S. W. Kuo, W. S. *Polymer.* **2010**, *51*, 3948-3955.
- Raza, A.; Si, Y.; Wang, X.; Ren, T.; Ding, B.; Yu, J.; Al-Deyab, S. S. *RSC Adv.* **2012**, *2*, 12804-12811.
- Liao, S. C.; Wang, F. C.; Lin, C. H.; Chou, Y. H.; Chang, C. F. *J. Phys. Chem. C.* **2008**, *112*, 16189-16191.
- Wang, F. C.; Chiou, F. S.; Ko, H. F.; Chen, K. J.; Chou, T. C.; Huang, F. C.; Kuo, W. S.; Chang, C. F. *Langmuir.* **2007**, *23*, 5868-5871.
- Liao, S. C.; Wu, S. J.; Wang, F. C.; Chang, C. F. *Macromol. Rapid Commun.* **2008**, *29*, 52-56.
- Kuo, W. S.; Liu, W. C. *J. Appl. Polym. Sci.* **2010**, *117*, 3121-3127.
- Huang, W. K.; Kuo, W. S. *Polymer Comp.* **2011**, *32*, 1086-1089.
- Takeichi, T.; Guo, Y.; Agag, T. *J. Appl. Polym. Sci.* **2000**, *38*, 4165-4176.
- Takeichi, T.; Y. Guo, Y. *Polym. J.* **2001**, *33*, 437-443.
- Takeichi, T.; Guo, Y.; Rimdusit, S. *Polymer.* **2005**, *46*, 4909-4916.
- Brunovska, Z.; Ishida, H. *J. Appl. Polym. Sci.* **1999**, *73*, 857-862.
- Kim, J. H.; Brunovska, Z.; Ishida, H. *Polymer.* **1999**, *40*, 1815-1822.
- Brunovska, Z.; Lyon, R.; Ishida, H. *Thermochim. Acta.* **2000**, *357*, 195-207.
- Agag, T.; Takeichi, T. *Macromolecules.* **2001**, *34*, 7257-7263.
- Agag, T.; Takeichi, T. *Macromolecules.* **2003**, *36*, 6010-6017.
- Yen, C. Y.; Cheng, C. C.; Chu, L. Y.; Chang, C. F. *Polym. Chem.* **2011**, *2*, 1648-1653.
- Hu, H. W.; K. W. Huang, W. K.; Kuo, W. S. *Polym. Chem.* **2012**, *3*, 1546-1554.
- Yagci, Y.; Kiskan, B.; L. A. Demirel, A. L.; Kamer, O. *J. Polym. Sci. Part A: Polym. Chem.* **2008**, *46*, 6780-6788.
- Demir, K. D.; Tasdelen, M. A.; Uyar, T.; Kawaguchi, A. W.; Sudo, A.; Endo, T.; Yagci, Y. *J. Polym. Sci. Part A: Polym. Chem.* **2011**, *49*, 4213-4220.
- Fu, K. H.; Huang, F. C.; Kuo, W. S.; Lin, C. H.; Yei, R. D.; Chang, C. F. *Macromol. Rapid Commun.* **2008**, *29*, 1216-1220.
- Kuo, W. S.; Chang, C. F. *Prog. Polym. Sci.* **2011**, *36*, 1649-1696.
- Chen, Q.; Xu, R.; Zhang, J.; Yu, D. *Macromol. Rapid Commun.* **2005**, *26*, 1878-1882.
- Liu, Y.; S. Zheng, S. *J. Polym. Sci., Part A: Polym. Chem.* **2006**, *44*, 1168-1181.
- Huang, M. J.; Kuo, W. S.; Huang, J. H.; Wang, X. Y.; Chen, Y. T. *J. Appl. Polym. Sci.* **2009**, *111*, 628-634.
- Hu, H. W.; Huang, W. K.; Chiou, W. C.; Kuo, W. S. *Macromolecules.* **2012**, *45*, 9020-9028.
- Xu, R.; Zhang, P.; Wang, J.; Yu, D.; Ishida, H.; Agag, T. “*Handbook of Polybenzoxazine*,” Eds., Elsevier, Amsterdam **2011**, Chapter 31, 541.
- Yang, C. C.; Wang, I. P.; Lin, C. Y.; Liaw, J. D.; Kuo, W. S. *Polymer.* **2014**, *55*, 2044-2050.
- Meng, F.; Ishida, H.; Liu, X. *RSC Adv.* **2014**, *4*, 9471-9475.

51. Kawaguchi, A. W.; Sudo, A.; Endo, T. *J. Polym. Sci. Part A: Polym. Chem.* **2014**, *52*, 410-416.
52. Szymanski, W.; Beierle, M. J.; Kistemaker, V. A. H.; Velema, A. W.; Feringa, L. B. *Chem. Rev.* **2013**, *113*, 6114-6178.
53. Jochum, D. F.; Theato, P. *Chem. Soc. Rev.* **2013**, *42*, 7468-7483.
54. Kim, D. H.; Ishida, H.; *J. Phys. Chem. A.* **2002**, *106*, 3271-3280.
- 10 55. Jiang, W.; Wang, G.; He, Y.; Wang, X.; An, Y.; Song, Y.; Jiang, L. *Chem. Commun.* **2005**, 3550-3552.
56. Low, Y. H.; Ishida, H. *Polym. Degrad. Stab.* **2006**, *91*, 805-815.
57. Lekesiz, O. T.; Hacaloglu, J. *Polymer* **2014**, *55*, 3533-3542.
- 15 58. Kuo, W. S.; Wu, H. C.; Chang, C. F. *Macromolecules.* **2004**, *37*, 192-202.
59. Pries, T. A.; C. Cheng, C.; Belfiore, A. L. *ACS. Proc. Div.; Polym. Mater. Sci. Eng.* **1989**, *61*, 466.
60. Kuo, W. S.; Huang, F.C.; Wu, H. C.; Chang, C. F. *Polymer.* **2004**, *45*, 6613-6620.
- 20 61. Liu, C.; Shen, D.; Sebastian, M. R.; Marquet, J.; Schonfeld, R. *Macromolecules.* **2011**, *44*, 4616-4622.
62. Wang, H. J.; Altukhov, O.; Cheng, C. C. Chang, C. F.; S. W. Kuo, W. S. *Polymers.* **2013**, *5*, 937-953.



**A Graphic Content:**

Azopyridine-functionalized benzoxazine (PBZ) was prepared and then blending with zinc ion through metal-ligand coordination to form high performance polybenzoxazine after thermal curing.

5